LA-UR-17-24947 (Accepted Manuscript)

Effects of MEA Fabrication and Ionomer Composition on Fuel Cell Performance of PGM-Free ORR Catalyst

Yin, Xi
Lin, Ling
Chung, Hoon Taek
Martinez, Ulises
Komini Babu, Siddharth
Purdy, Geraldine Maxine
Zelenay, Piotr

To be published in: ECS Transactions

DOI to publisher's version: 10.1149/07711.1273ecst

Permalink to record: http://permalink.lanl.gov/object/view?what=info:lanl-repo/lareport/LA-UR-17-24947

Effects of MEA Fabrication and Ionomer Composition on Fuel Cell Performance of PGM-free ORR Catalyst

X. Yin,[1] L. Lin,[1,2] H.-T. Chung, S. Komini Babu, U. Martinez, G. M. Purdy, and P. Zelenay[*]

Materials Physics and Applications Division, Los Alamos National Laboratory, Los Alamos, New Mexico, 87544, USA

Carbon-based platinum group metal-free (PGM-free) catalysts for oxygen reduction reaction (ORR) have received increasing attention as potential candidates for low-cost fuel cell cathode catalysts. Mass-transport within the very thick catalyst layer (CL) presents a major challenge to further improve the fuel cell performance of PGM-free catalysts, which may be realized through the optimization of CL structure. Herein, we demonstrate that membrane electrode assemblies (MEAs) with not hot-pressed PGM-free cathode showed improved H_2-air fuel cell performance in mass transport region when compared to MEAs prepared via hot-pressing technique. Further, the effects of the ionomer content and equivalent weight (EW) on fuel cell performance were systematically explored. We observed that an increase in ionomer content resulted in performance improvement in the kinetic region, while negatively affecting the performance in the mass transport region. The overall optimum fuel cell performance was achieved with an ionomer EW of 830 g mol^{-1}.

Introduction

Platinum group metal-free (PGM-free) oxygen reduction reaction (ORR) catalysts synthesized from earth-abundant elements such as carbon, nitrogen, and transition metals are promising alternatives to Pt-based catalysts in the cathode of polymer electrolyte fuel cells (PEFCs). Significant interest over the past decade has led to notable improvements in the activity and durability of PGM-free catalysts (1-5). The low volumetric activity of PGM-free catalysts requires high catalyst loading in order to achieve sufficient current density, resulting in catalyst layers (CLs) *ca.* 100 μm thick, about one order of magnitude thicker than Pt-based CLs. The CL morphology and composition of the generally very thick PGM-free electrode has significant impact on fuel cell performance, affecting oxygen and proton transport. However, unlike well-optimized Pt-based CLs, there have been very few studies reported on the optimization of PGM-free CLs to date (6, 7).

In a fuel cell, a thick catalyst layer (> 100 μm) is amenable to increased mass transport resistance and liquid-water flooding (8). In order to mitigate these effects, CLs with higher porosity and lower transport resistance are favored. Increasing the CL porosity reduces the gas transport resistance and facilitates the removal of water in the hydrophilic

[1] X. Y. and L. L. contributed equally to this work.

[2] Visiting scholar from Division of Nanomaterials and Chemistry, Hefei National Laboratory for Physical Science at Microscale, University of Science and Technology of China, Hefei, Anhui, 230026, China.

PGM-free catalyst layer (8). On the other hand, high CL porosity results in increased tortuosity, which in turn enhances the ionic resistance within the CL (9). For similar catalyst loadings, increasing the porosity also makes the CL thicker. Therefore, optimization of the CL morphology is crucial to achieving a balance between the effective mass transport properties and food proton conductivity. Hot-pressing is a common method of fabricating MEAs and has been used to establish good contact between the CL and the membrane; however, this common methodology inevitably lowers the CL porosity. In a catalyst-coated membrane (CCM), the catalyst is directly deposited on the membrane, enhancing the contact between the membrane and the CL. It has been reported that hot-pressing a CCM when fabricating an MEA can increase the performance for some Pt-based cathodes (10, 11). In the case of the PGM-free electrode, the hierarchical porosity of PGM-free catalysts aid with the removal of liquid water and transport of the reacting gas (8). Nevertheless, this pore connectivity is shown to be compromised upon hot-pressing (7).

It has been observed that the performance of the PGM-free electrode is significantly affected by the ionomer distribution and loading (8). Ionomer loading affects the extent of infiltration into the micropores of the PGM-free catalyst agglomerates. Unlike the Pt-based catalysts, the active sites of the PGM-free catalyst are distributed throughout the carbon surface, which is composed mostly of microporous carbon structures. Therefore, ionomer infiltration into the micropores is necessary for protons to access the active sites. The level of infiltration into the micropores also influences the hydrophilicity of the CL and increases the gas transport resistance (8). Ionomer distribution, which is also controlled by the ionomer loading, impacts the proton conductivity and, hence, the ohmic overpotential. For the Pt-based cathode, a decrease in the ionomer content leads to a reduction in proton conductivity, and excessive ionomer limits the gas diffusion and removal of water. Previous work from our group has shown the effect of ionomer loading on the kinetic region of the polarization plot (8). In addition, ionomer equivalent weight (EW) affects the proton conductivity and mass transport properties. The effect of ionomer content and EW on Pt-based cathodes has been widely investigated (12-14). At low ionomer loading, Pt-based electrodes with low-EW ionomer exhibit better performance. However, the microstructure of carbon and active-site distribution in PGM-free catalysts differs greatly from Pt-based catalysts, affecting the mass transport phenomena within the CL requiring further optimization of the ionomer content and EW.

In this work, we present the effect of the hot-pressing process during MEA fabrication on the fuel cell performance of highly porous PGM-free cathodes. Further, the effects on H_2-air fuel cell performance of ionomer content and EW were systematically explored by employing three different ionomers (EW of 720, 830, and 1100 g/mol SO_3H), at varied contents ranging from 25 wt% to 55 wt%.

Experimental

Catalyst and ink preparation

The PGM-free catalyst used in this paper was prepared by high-temperature pyrolysis of nitrogen precursors (cyanamide and polyaniline), iron precursor ($FeCl_3$) and carbon support (Black Pearl 2000) combined with a pore-forming agent ($ZnCl_2$), followed by acid leaching, magnetic separation using a permanent magnet and a second pyrolysis (15,

16). Catalyst inks were prepared by mixing 30 mg of the catalyst with various amounts of ionomer dispersions in a solvent containing water and isopropanol and sonicating in an ultrasonic bath for 4 to 5 h. The ionomer dispersions used were 5 wt% Nafion® D521 (EW 1100 g/mol SO_3H, Alfa Aeser), 24 wt% Aquivion® D83-24B (EW 830 g/mol SO_3H, Sigma-Aldrich) and 25 wt% Aquivion® D72-25BS (EW 720 g/mol SO_3H, Sigma-Aldrich). Four inks with varying ionomer content from 25 wt% to 55 wt% were made for each ionomer.

Membrane electrode assembly (MEA) fabrication

Scheme 1 illustrates the two MEA fabrication methods. For MEA fabricated with hot-pressing, the catalyst ink was hand-brushed onto a Nafion® NR211 membrane at ~ 80 ºC to make a 5 cm^2 electrode with a catalyst loading of *ca.* 4.8 mg/cm^2. Then, MEA was obtained by hot-pressing a gas diffusion layer (GDL, 29BC, Ion Power) onto the cathode catalyst layer and a 0.3 mg_{pt} cm^{-2} anode (a gas diffusion electrode, GDE, Fuel Cell Store) on the other side of the membrane at 120 ºC for 5 min using a pressure of *ca.* 5.3 MPa. For MEA fabricated without hot-pressing the cathode, a the anode GDE was first hot-pressed to one side a Nafion® NR211 membrane at 120 ºC, 5.3 MPa for 5 min. The catalyst ink was then brush-painted to the cathode side of the membrane at ~ 80 ºC to achieve a same catalyst loading of *ca.* 4.8 mg/cm^2. In both cases, the MEAs were assembled by adding GDLs on top of the cathode CL. PTFE gaskets were used to control the compression of MEAs in fuel cell hardware to *ca.* 75% to 80% of its original thickness.

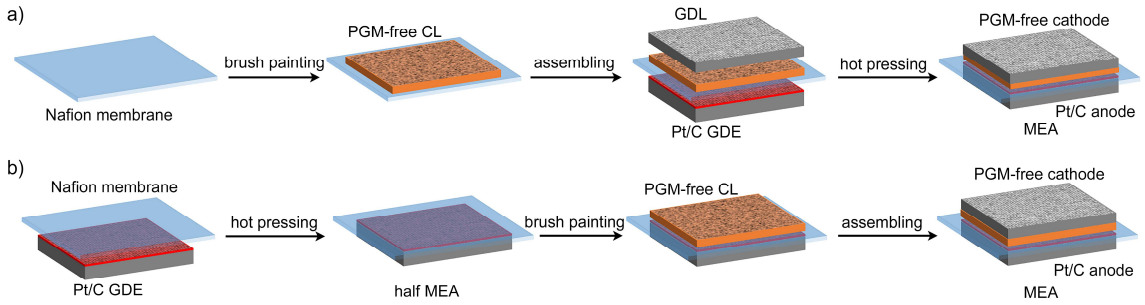

Scheme 1. Two MEA fabrication methods used in this research.

Fuel cell testing and cathode cyclic voltammetry

Single-cell performance was measured in H_2-air fuel cell with fully humidified H_2 and air, both at a flow rate of 200 sccm and 100% relative humidity (RH). The cell temperature was 80 ºC. 10.2 psig backpressure was applied to maintain 1.0 bar partial pressure of H_2 and a total of partial pressures of oxygen and nitrogen in air, corresponding to 0.2 bar O_2 partial pressure, at the Los Alamos altitude. The polarization plots were recorded from open circuit voltage (OCV) to 0.2 V at either a step of 0.05 V with step period of 30 s or a step of 0.02 V with step period of 10 s.

The oxygen-free cyclic voltammograms for the PGM-free cathodes were measured on a CHI 760d potentiostat (CH Instruments) after measuring the polarization plot and flushing cathode with N_2 for 10 min. The anode was used as a counter/quasi-reference

electrode. Fully humidified H_2 and N_2 were flown at 200 sccm and atmospheric pressure through the anode and cathode, respectively. The cyclic voltammograms were recorded from 0 to 1.0 V *vs*. RHE at a scan rate of 20 mV/s. A constant capacitance of 30 μF/cm^2 was employed to estimate the electrochemical surface area (ECSA) of PGM-free catalyst in the cathode.

Results and Discussion

Effect of the MEA fabrication method

Figure 1 shows an SEM micrograph of the cross-section of a typical MEA with a PGM-free cathode and a Pt/C anode. The thickness of the PGM-free CL is approximately 100 μm, much thicker than the Pt/C CL at the anode, which is approximately 10 μm. Figure 2 shows the SEM micrographs of MEAs with PGM-free CL prepared with and without hot-pressing, at the same catalyst loading of *ca*. 4.8 mg/cm^2. The not hot-pressed PGM-free CL is approximately 30-40 μm thicker than the hot-pressed CL, implying that it is less compressed and thus contains a larger volume of pores. The higher electrode porosity in PGM-free CL may favor the mass transport of air and water, and improve the fuel cell performance.

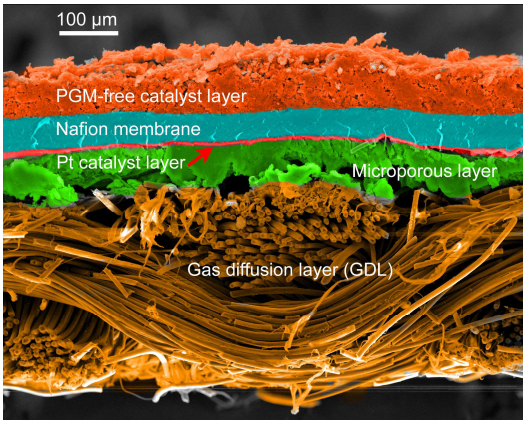

Figure 1. SEM micrographs of an MEA cross section with PGM-free cathode and Pt/C anode. False colors applied for clarity.

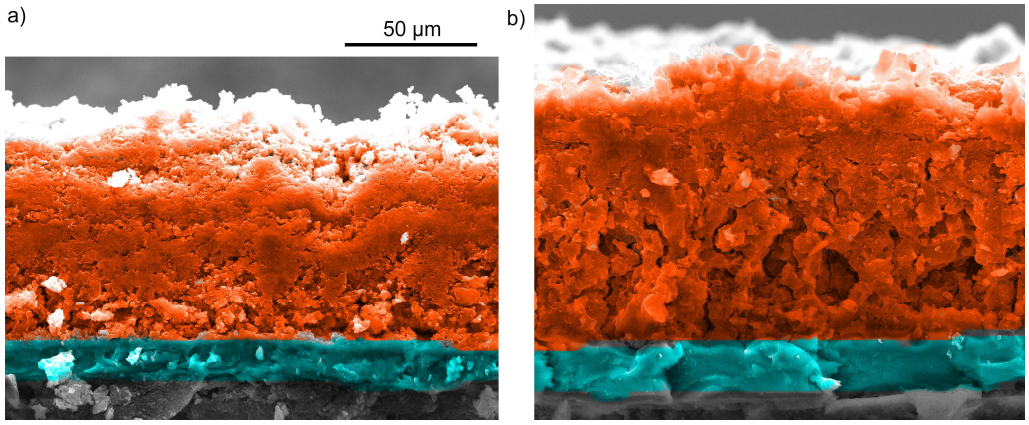

Figure 2. SEM micrographs of the cross sections of PGM-free cathodes fabricated (a) with hot-pressing and (b) without hot-pressing. False colors applied for clarity.

Figure 3 shows the polarization plots with the cathodes fabricated by the CCM method with and without hot-pressing. It can be observed that hot-pressed MEAs suffer from performance loss at high current densities due to higher mass transport resistance, which becomes more severe when using an ionomer with lower EW (Figure 3b). On the other hand, MEA fabricated without the hot-pressing show improved performance at both ohmic and mass transport regions. Although the high-frequency resistance (HFR) of the not hot-pressed MEA is greater than that of hot-pressed MEA, the measured current density in the kinetic region are identical for both MEAs. These results suggest that not hot-pressing benefits the kinetic performance by providing better O_2 accessibility to active sites.

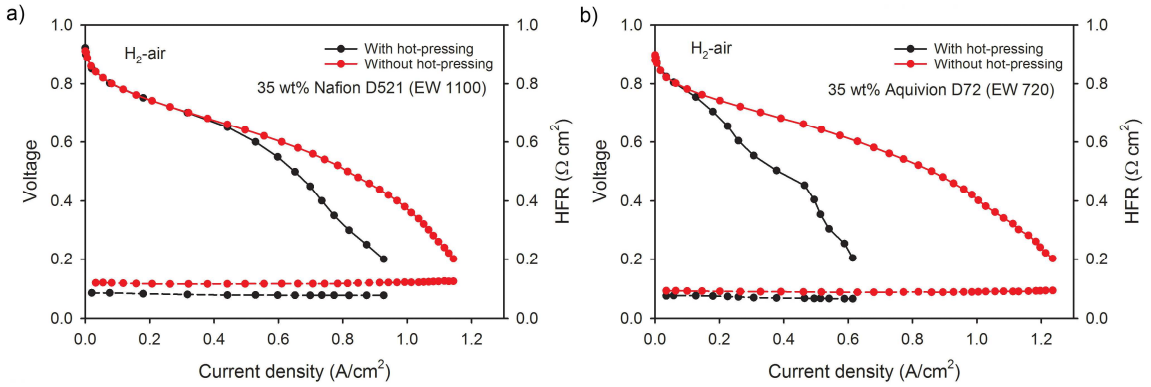

Figure 3. Comparison of the H_2-air fuel cell performance of MEAs with PGM-free cathodes fabricated with and without hot-pressing using different ionomers: (a) 35 wt% Nafion®; (b) 35 wt% Aquivion® D72. Cathode: PGM-free catalyst, *ca*. 4.8 mg/cm^2, 1.0 bar air partial pressure, 200 sccm; anode: Pt/C, 0.3 mg$_{Pt}$/cm^2, 1.0 bar H_2 partial pressure, 200 sccm; cell temperature 80 ºC, 100% RH; Nafion® NR211 membrane.

Effects of ionomer loading and EW

The effects of the ionomer loading and EW on fuel cell performance were systematically studied utilizing three ionomers of different EWs, Nafion® D521 (EW 1100), Aquivion® D83 (EW 830) and Aquivion® D72 (EW 720), with various ionomer contents (25 wt%, 35 wt%, 45 wt%, and 55 wt%). Figure 4 shows the polarization plots of MEAs containing different Nafion® D521 contents. Fuel cell performance at the kinetic region increases with an increase in the ionomer loading. When Nafion® content was 25 wt%, the kinetic and ohmic performance is much lower than with other ionomer contents, indicating that the proton conductivity and catalyst utilization of catalyst layer with 25 wt% of Nafion® are insufficient. The kinetic performance enhances with 35 wt% to 55 wt% of Nafion®, while limits in mass transport region become more significant. However, thanks to the more porous electrode structure, the mass transport limitations at high ionomer loading is alleviated compared to previously reported results obtained with the hot-pressed PGM-free CL (17), and high current density is achieved at a Nafion® loading of 55 wt%.

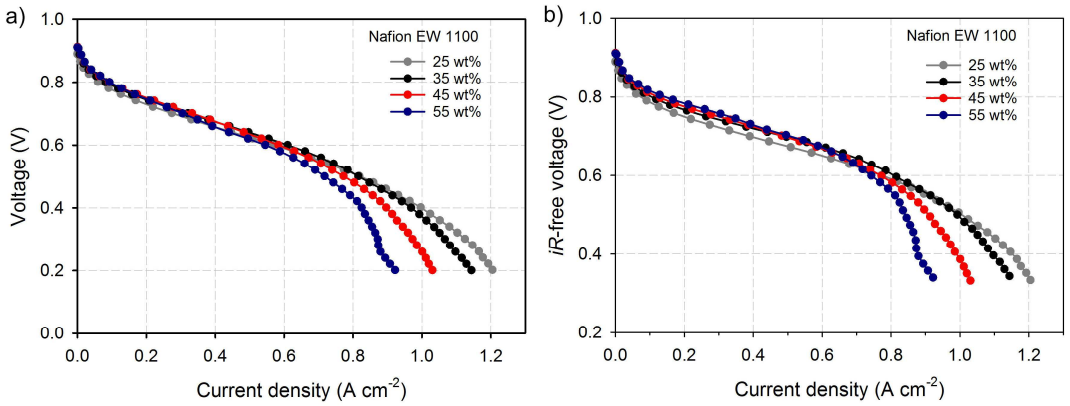

Figure 4. Comparison of H_2-air fuel cell performance of MEAs with not hot-pressed PGM-free cathodes containing different content of Nafion® (EW 1100): (a) Polarization curve; (b) *iR*-free polarization curve. Cathode: PGM-free catalyst, *ca*. 4.8 mg/cm^2, 1.0 bar air partial pressure, 200 sccm; anode: Pt/C, 0.3 mg_{Pt}/cm^2, 1.0 bar H_2 partial pressure, 200 sccm; cell temperature 80 ºC, 100% RH; Nafion® NR211 membrane.

Figure 5 shows the dependency of fuel cell performance on the EW and the content of ionomer in two-dimensional (2D) contour graphs. To evaluate fuel cell performance, *iR*-free current density at 0.8 V and measured current density at 0.65 V were chosen as the performance indicators. As an indicator of kinetic performance, *iR*-free current density at 0.8 V increases with an increase in the ionomer content (Figure 5a). In practice, taking power output and energy consumption into account, most fuel cell developers use between 0.6 V and 0.7 V as the voltage at nominal power (18). Therefore, the current density at 0.65 V is a practical parameter to evaluate the overall fuel cell performance. Figure 5b shows that the best fuel cell performance at 0.65 V is achieved at moderate ionomer loadings, 35 wt% or 45 wt%, with all tested ionomers, indicating the emerging impact of mass transport resistance at 0.65 V. Among three tested ionomers, Aquivion® D83 with an EW value of 830 g mol^{-1} yields the most balanced fuel cell performance.

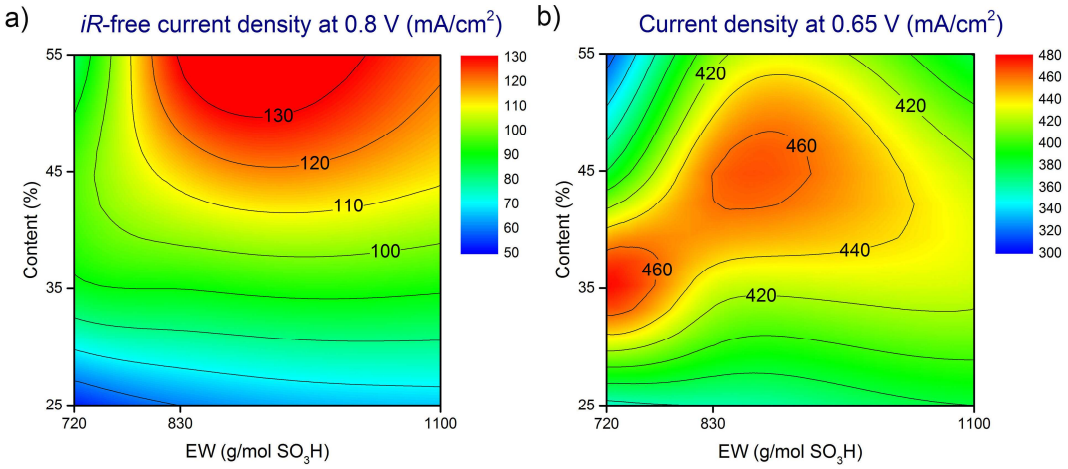

Figure 5. Two-dimensional graphs showing the relationship between fuel cell performance and two ionomer-related variables (EW and loading) from MEAs with not hot-pressed cathode: (a) *iR*-free current density at 0.8 V, and (b) current density at 0.65 V. Cathode: PGM-free catalyst, *ca*. 4.8 mg/cm^2, 1.0 bar air partial pressure, 200 sccm; anode: Pt/C, 0.3 mg_{Pt}/cm^2, 1.0 bar H_2 partial pressure, 200 sccm; cell temperature 80 ºC, 100% RH; Nafion® NR211 membrane.

Figure 6 shows cyclic voltammograms of cathode CLs with different content of Nafion® (EW 1100). The results demonstrate that double layer capacitance increases when increasing the ionomer content. Since the same catalyst loading was used throughout this study, the increased cathode double layer capacitance implies an increase in the electrochemical surface area with an increase in the ionomer content or, in other words, an increase in the utilization of PGM-free catalyst with an increase in the ionomer content. Figure 7a summarized the dependency of ECSA on the ionomer EW and content. In all cases, ECSA increases with an increase in the ionomer content, implying that the catalyst utilization could be increased by increasing ionomer content. At the same ionomer content, ECSA also increases with an increase in the ionomer EW. Figure 7b shows the correlation between the ECSA and fuel cell performance in the kinetic region, expressed as the *iR*-free current density at 0.8 V. A very good correlation is observed between ECSA and fuel cell performance at that voltage.

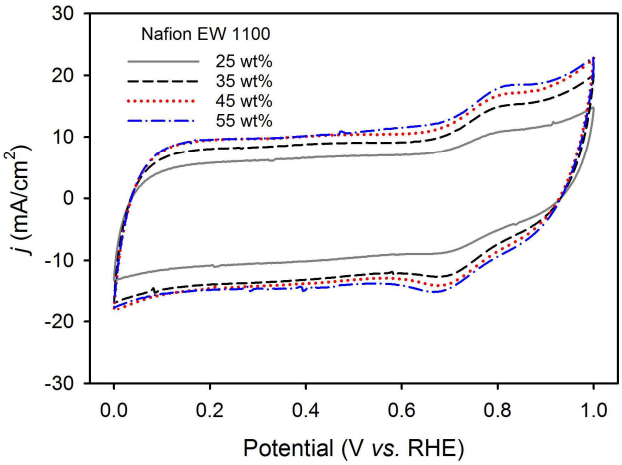

Figure 6. Cyclic voltammetry of not hot-pressed PGM-free cathodes with different Nafion® loadings.

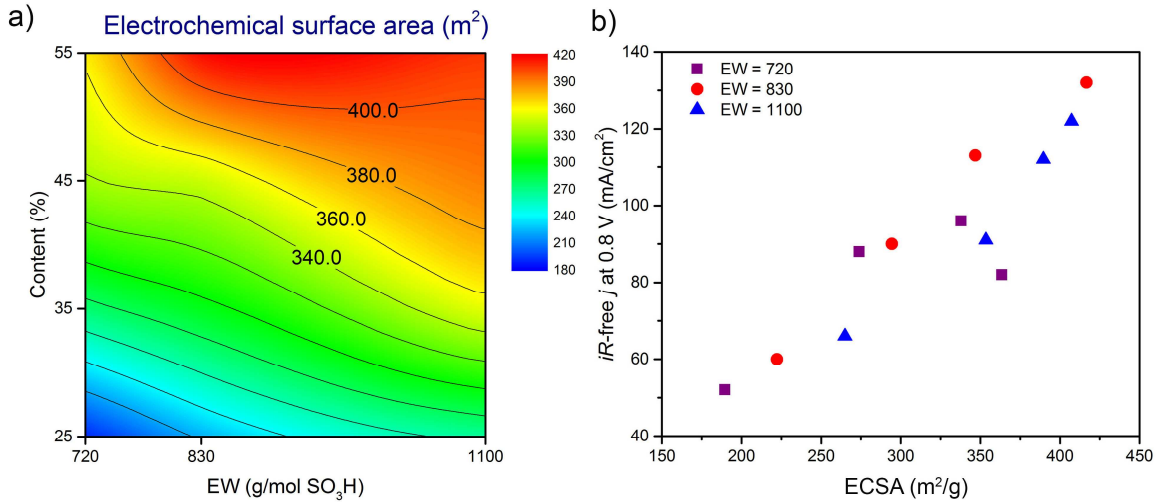

Figure 7. (a) Two-dimensional graph showing the relationship between ECSA estimated from double layer capacitance and two ionomer-related variables (EW and loading) from MEAs with not hot-pressed cathode. (b) Correlation between *iR*-free current density at 0.8 V and ECSA of PGM-free cathodes.

Conclusions

MEAs fabricated with a not hot-pressed PGM-free cathode showed higher H_2-air fuel cell performance than those prepared by the common hot-pressing approach. The most significant improvement was observed in the mass transport region. This is being attributed to maintaining higher electrode porosity by not hot-pressing the MEA, which results in lower mass transport resistance. Higher ionomer content in catalyst layer improved the utilization of the PGM-free catalyst, ensuring better performance in the kinetic region. However, higher ionomer content worsens mass transport leading to flooding issues. For the same ionomer content, an increase in EW increased performance in the kinetic region. Therefore, the most balanced MEA performance is achieved with middle range of ionomer content at 35 wt% to 45 wt%. Among the three ionomers with different EW, the use of ionomer with 830 EW yielded the most satisfying overall performance in fuel cell testing.

Acknowledgments

Financial support for this research by DOE-EERE through Fuel Cell Technologies Office is gratefully acknowledged. The author would like to thank Dr. Natalia Macauley and Dr. Tommy Rockward at LANL for helpful discussion.

References

1. G. Wu, K. L. More, C. M. Johnston and P. Zelenay. *Science* **332**, 443-447 (2011).
2. G. Wu and P. Zelenay. *Acc. Chem. Res.* **46**, 1878-1889 (2013).
3. E. Proietti, F. Jaouen, M. Lefèvre, N. Larouche, J. Tian, J. Herranz and J.-P. Dodelet. *Nat. Commun.* **2**, 416 (2011).
4. X. Wang, H. Zhang, H. Lin, S. Gupta, C. Wang, Z. Tao, H. Fu, T. Wang, J. Zheng, G. Wu and X. Li. *Nano Energy* **25**, 110-119 (2016).
5. P. Zelenay In *Non-precious metal fuel cell cathodes: Catalyst development and electrode structure design*, US Department of Energy, Energy Efficiency and Renewable Energy, Annual Merit Review meeting., 2016.
6. D. Malko, T. Lopes, E. A. Ticianelli and A. Kucernak. *J. Power Sources* **323**, 189-200 (2016).
7. S. Stariha, K. Artyushkova, M. J. Workman, A. Serov, S. McKinney, B. Halevi and P. Atanassov. *J. Power Sources* **326**, 43-49 (2016).
8. S. Komini Babu, H. T. Chung, P. Zelenay and S. Litster. *ACS Applied Materials & Interfaces* **8**, 32764-32777 (2016).
9. S. Litster and G. McLean. *J. Power Sources* **130**, 61-76 (2004).
10. Q. Meyer, N. Mansor, F. Iacoviello, P. L. Cullen, R. Jervis, D. Finegan, C. Tan, J. Bailey, P. R. Shearing and D. J. L. Brett. *Electrochim. Acta* **242**, 125-136 (2017).
11. M. Yazdanpour, A. Esmaeilifar and S. Rowshanzamir. *Int. J. Hydrogen Energy* **37**, 11290-11298 (2012).
12. Y. Liu, C. Ji, W. Gu, D. R. Baker, J. Jorne and H. A. Gasteiger. *J. Electrochem. Soc.* **157**, B1154-B1162 (2010).
13. Y.-C. Park, H. Tokiwa, K. Kakinuma, M. Watanabe and M. Uchida. *J. Power Sources* **315**, 179-191 (2016).
14. A. Orfanidi, P. Madkikar, H. A. El-Sayed, G. S. Harzer, T. Kratky and H. A. Gasteiger. *J. Electrochem. Soc.* **164**, F418-F426 (2017).

15. L. Lin, H. T. Chung, X. Yin, U. Martinez and P. Zelenay. *Meeting Abstracts* **MA2016-02**, 2826 (2016).
16. X. Yin, U. Martinez, H. T. Chung, L. Lin and P. Zelenay. *Meeting Abstracts* **MA2016-02**, 2672 (2016).
17. S. Komini Babu, H. T. Chung, P. Zelenay and S. Litster. *ECS Transactions* **69**, 23-33 (2015).
18. F. Barbir, Chapter Five - Fuel Cell Operating Conditions. In *PEM Fuel Cells (Second Edition)*, Academic Press: Boston, pp 119-157 (2013).